

Nonlinear spherical gravitational downfall of gas onto a solid ball: analytic and numerical results

José Gaite

*Instituto de Matemáticas y Física Fundamental, CSIC,
Serrano 123, 28006 Madrid, Spain*

and

Mari-Paz Zorzano

*Centro de Astrobiología, CSIC-INTA,
Carretera de Torrejón a Ajalvir, 28850 Torrejón de Ardoz, Madrid, Spain.*

May 14, 2003

Abstract

The process of downfall of initially homogeneous gas onto a solid ball due to the ball's gravity (relevant in astrophysical situations) is studied with a combination of analytic and numerical methods. The initial explicit solution soon becomes discontinuous and gives rise to a shock wave. Afterwards, there is a crossover between two intermediate asymptotic similarity regimes, where the shock wave propagates outwards according to two self-similar laws, initially accelerating and eventually decelerating and vanishing, leading to a static state. The numerical study allows one to investigate in detail this dynamical problem and its time evolution, verifying and complementing the analytic results on the initial solution, intermediate self-similar laws and static long-term solution.

PACS: 47.40.-x, 47.70.Nd, 98.35.Mp

1 Introduction

The problem of unsteady motion of compressible gas giving rise to the formation of shock waves has been the subject of continuing attention. In particular, the polytropic gas flow in one dimension is amenable to powerful mathematical methods [1, 2, 3]. The introduction of gravitational forces complicates the problem but widens its range of applications.

We study in this paper a dynamical problem that is very simple to formulate: given a solid body with a spherically symmetric mass distribution (a ball), placed in a homogeneous gas, analyze the subsequent evolution of this gas under the body's gravity. This problem has applications in several astrophysical situations involving gas accretion. For example, it could be a simplified model for the formation of planetary atmospheres: as a result

of gas accretion onto the solid (rock) surface of a previously formed spherical core, an atmosphere may form. Alternatively, it could represent the downfall of gas onto a neutron star. The problem leads to solving the partial differential equations of fluid dynamics in one dimension (the radial distance). These equations are nonlinear and no general method of solution is available. However, given the simplicity of the initial and boundary conditions, many results can be obtained by purely analytic means (as we shall see). The numerical integration of the partial differential equations provides an alternative method of study which is used here to validate and complement the analytic results.

Certain aspects of this fluid dynamical problem have been treated before in the astrophysical literature [4, 5]. However, a complete treatment employing the full power of nonlinear fluid dynamics methods has not yet been attempted. The thorough analytic and numerical treatment provided here allows one to attain a picture of the whole process and to connect with other problems in fluid dynamics, especially, with gravitation. In particular, the exact description of the formation of the shock wave may illustrate general features present in other processes.

This paper is organized as follows. In section 2, we introduce the relevant magnitudes of the problem to get an intuitive idea of the physics involved. Afterwards, we introduce the fluid equations to be used. In section 3, an exact solution is found for the initial non-trivial dynamics, which occurs near the ball's surface. In the following sections we obtain two *similarity* solutions valid for larger t , the first still confined within a small height (section 4), while the second is valid for large radius (section 5). In section 6 we integrate numerically the partial differential equations of the constant gravity and varying gravity case and compare the numerical results with the analytical ones. Finally, in section 7, we consider the long-time asymptotic static state and explore the transition to it with the numerical solution. In section 8 we summarize and discuss the results.

2 Relevant magnitudes and fluid equations

The initial condition, namely, the (spherically symmetric) solid ball in the homogeneous gas, is characterized by four parameters: the radius R and mass M of the ball, and the pressure P_0 and density ρ_0 of the gas (we assume that the gas is perfect, inviscid, and polytropic). In addition, we have the constant of gravity G . From these five dimensional characteristic parameters, we can form two independent dimensionless numbers: the ratio of densities $(4/3)\pi R^3(\rho_0/M)$ and the ratio $RP_0/(\rho_0 GM)$. The quantity $P_0/\rho_0 \sim c_0^2$ (c_0 being the sound speed) is approximately the gas thermal energy per unit of mass. On the other hand, GM/R is the gas potential energy per unit of mass on the ball. Their ratio measures the relative strength of gravity in our problem. To have any significant gas downfall, we must demand that the ball's gravity dominates over the gas thermal energy, that is, $Rc_0^2/(GM) \ll 1$.

Defining the scale at which the gas thermal energy is similar to its potential energy as $\mathcal{R} = GM/c_0^2$, we demand that

$$R \ll \mathcal{R} \ll \left(\frac{M}{\rho_0}\right)^{1/3}. \quad (1)$$

The last length is the radius of a volume of gas such that its mass is similar to M and, therefore, we can neglect the self-gravity of the gas.

Since the initial and boundary conditions are spherically symmetric, we will assume that the whole process is spherically symmetric and thus one-dimensional. We further consider an adiabatic evolution of the gas or, more generally, a *polytropic* equation of state, $P \propto \rho^\gamma$ ($\gamma \geq 1$): for a perfect gas, with $\gamma = C_P/C_V$ (the constant ratio of specific heats), a polytropic process is adiabatic, but the notion of polytropic process is more general. For numerical calculations, we will use $\gamma = 7/5$ (the adiabatic index of a perfect diatomic gas). Then, we have the continuity equation, the Euler equation and the thermodynamic equation:

$$\frac{\partial \rho}{\partial t} + \frac{\partial(\rho v)}{\partial x} + \frac{2(\rho v)}{x+R} = 0, \quad (2)$$

$$\frac{\partial v}{\partial t} + v \frac{\partial v}{\partial x} = -g(x) - \frac{1}{\rho} \frac{\partial P}{\partial x}, \quad (3)$$

$$\frac{\partial P}{\partial t} \frac{1}{\rho^\gamma} + v \frac{\partial P}{\partial x} \frac{1}{\rho^\gamma} = 0, \quad (4)$$

where x is the radial distance from the ball surface and $g(x) = GM/(x+R)^2 = gR^2/(x+R)^2$ is the gravity acceleration (g is the gravity at the ball surface). The initial conditions are: $\rho(0, x) = \rho_0$, $P(0, x) = P_0$ and $v(0, x) = 0$ ($x \geq 0$). The boundary condition at the solid surface is $v(t, 0) = 0$. We remark that the behaviour of the solutions of these equations for large x is only determined by the initial conditions, which in some sense replace a boundary condition “at infinity”. However, in the numerical calculations we shall need a real boundary condition at some large value of x .

The thermodynamic equation (4) (which expresses conservation of entropy or some more general thermodynamic quantity) has the trivial solution $P/\rho^\gamma = P_0/\rho_0^\gamma$. Introducing the sound velocity c ($c^2 = dP/d\rho$), we can write the preceding solution as

$$c^2(\rho)/c_0^2 = (\rho/\rho_0)^{\gamma-1} \quad (c_0^2 = \gamma P_0/\rho_0). \quad (5)$$

Therefore, we need to consider only the two remaining equations:

$$\frac{\partial \rho}{\partial t} + \frac{\partial(\rho v)}{\partial x} + \frac{2(\rho v)}{x+R} = 0, \quad (6)$$

$$\frac{\partial v}{\partial t} + v \frac{\partial v}{\partial x} = -g(x) - \frac{c^2(\rho)}{\rho} \frac{\partial \rho}{\partial x}. \quad (7)$$

However, in the presence of a shock discontinuity, the thermodynamic equation (4) breaks down (as is most intuitive when this equation can be interpreted as entropy conservation). Therefore, the solution (5) does not hold, as we shall see in the numerical solution.

The fluid equations can also be derived as conservation equations, namely, as equations for conservation of mass, momentum and energy. In our case, we need to take into account that x is the radial distance and write the divergences in spherical coordinates; in particular, the divergence of the stress tensor $T^{ij} = \rho v^i v^j + g^{ij} P$ (g^{ij} is the inverse metric). The fluid

equations in conservative form become:

$$\frac{\partial \rho}{\partial t} + \frac{\partial [(x+R)^2 \rho v]}{(x+R)^2 \partial x} = 0, \quad (8)$$

$$\frac{\partial(\rho v)}{\partial t} + \frac{\partial [(x+R)^2 \rho v^2]}{(x+R)^2 \partial x} + \frac{\partial P}{\partial x} = -g(x)\rho, \quad (9)$$

$$\frac{\partial(\rho e + \rho v^2/2)}{\partial t} + \frac{\partial [(x+R)^2(\rho e + \rho v^2/2 + P)v]}{(x+R)^2 \partial x} = -g(x)\rho v. \quad (10)$$

They are equivalent to Eqs. (2,3,4), provided that the pressure is related with the internal energy (per unit mass) e by $P = (\gamma - 1)\rho e$ and that the solutions are smooth. In the presence of a shock discontinuity, the conservation equations still hold, which is their main advantage. Their disadvantage is that they are more complicated.

Defining the vector $\mathbf{U} = (\rho, \rho v, \rho e + \rho v^2/2)$, we can express the equations in the following divergence form:

$$\frac{\partial \mathbf{U}}{\partial t} + \frac{\partial \mathbf{F}(\mathbf{U})}{\partial x} = \mathbf{G}(\mathbf{U}), \quad (11)$$

with $\mathbf{F}(\mathbf{U}) = (\rho v, \rho v^2 + P, (\rho e + \rho v^2/2 + P)v)$ and $\mathbf{G}(\mathbf{U}) = (-2\rho v/(x+R), -2\rho v^2/(x+R) - g(x)\rho, -2(\rho e + \rho v^2/2 + P)/(x+R) - g(x)\rho v)$ the source term. This form will be useful in the next section, and for numerical calculations as well.

3 Early stage: exact solution

Initially, the gas will start falling with acceleration $g(x)$, that is, with a negative velocity increasing as $v \sim -g(x)t$. However, it will be stopped at the ball's surface, where the density and, therefore, the pressure must increase. Consequently, a wave transmitting the boundary condition $v(t, 0) = 0$ will propagate outwards. It is therefore crucial to determine the law of propagation of waves in the present conditions. This is called, in mathematical terms, the analysis of *characteristics*. Once this is done, and as long as the dynamics consists of the propagation of a *simple wave*, one can obtain an exact solution. We do not have here the opportunity to review the theory of simple waves, so we provide some indications and refer the reader to general treatises on the theory of one-dimensional gas flow for a comprehensive treatment [1, 2, 3].

For the moment, we confine ourselves to a spherical shell over the surface of height much smaller than R , where we can consider constant $g = GM/R^2$. Hence, the problem becomes that of the fall of gas on a flat surface (the ground). So we must use the one-dimensional form of the vector divergence and, therefore, we must neglect the last term on the left-hand side of the continuity equation (6), writing it as

$$\frac{\partial \rho}{\partial t} + \frac{\partial(\rho v)}{\partial x} = 0. \quad (12)$$

The gas still unperturbed by the wave merely falls with velocity $v = -gt$. In a reference system falling with it, it is at rest and, therefore, the speed of sound is c_0 . Hence, in the

original reference system the wave front is located at $x_f = c_0 t - g t^2/2$. Then, for $x > x_f$, the solution is trivial, and we only have to find the solution for $x < x_f$. In the falling frame, the acceleration of gravity vanishes and the set of two equations (12) and (7) reduces to a “gas tube problem” that can be solved by introduction of the Riemann invariants [1, 2, 3].

The Riemann invariants are best introduced by writing the equations in the divergence form (11). The replacement of spherical geometry with cartesian geometry reduces the source term to $\mathbf{G}(\mathbf{U}) = (0, -g\rho, -g\rho v)$ and, furthermore, the change to the falling frame removes it. Then we can write the divergence form (11) as a quasilinear partial differential equation:

$$\frac{\partial \mathbf{U}}{\partial t} + A(\mathbf{U}) \cdot \frac{\partial \mathbf{U}}{\partial x} = 0, \quad (13)$$

where $A(\mathbf{U})$ is the Jacobian matrix of derivatives of $\mathbf{F}(\mathbf{U})$ with respect to \mathbf{U} . The solution of this equation is carried out by diagonalizing A : the eigenvalues λ of A (which are real because the equations are hyperbolic) define the *characteristic curves*

$$\frac{dx}{dt} = \lambda(\mathbf{U}), \quad (14)$$

and the left eigenvectors of A (the eigenvectors of its transpose) define the Riemann invariants J , that is, functions that satisfy

$$A(\mathbf{U})^T \cdot \frac{\partial J}{\partial \mathbf{U}} = \lambda \frac{\partial J}{\partial \mathbf{U}} \quad (15)$$

for some eigenvalue λ . It is easy to prove that J is constant along the characteristic associated with the corresponding λ . The characteristics are the directions of propagation of disturbances (waves). Since we have three eigenvalues, namely, v and $v \pm c$, we have that the first family of characteristics are the streamlines and the other two families are forward or backward characteristics, according to the sign.

Let us denote x', v', c' the coordinate and variables in the falling frame. Initially we have a *constant state* (with v' and P constant), which is preserved for $x' \geq c_0 t$. Therefore, the backward characteristics crossing the forward characteristic $x' = c_0 t$ transmit a constant value of the Riemann invariant J_- , so the solution is a forward simple wave. Given that

$$J_- = v' - \frac{2c'}{\gamma - 1} = -\frac{2c_0}{\gamma - 1},$$

the sound velocity is related with the gas velocity by $c' = c_0 + (\gamma - 1)v'/2$. Furthermore, the fact that the solution is a forward simple wave implies that the forward characteristics are straight lines (see Fig. 1). Hence, the wave’s propagation law $v' = F[x' - (v' + c')t]$ is an implicit equation for v' , assuming that we can determine the function F . This is done using the boundary condition $v(t, 0) = 0$. The implicit equation is algebraic and its solution is straightforward. We then obtain:

$$v(x, t) = \begin{cases} -gt, & x \geq c_0 t - \frac{g}{2}t^2 \\ -\frac{c_0}{\gamma} - \frac{\gamma - 1}{2\gamma}gt + \sqrt{\left(\frac{c_0}{\gamma} + \frac{\gamma - 1}{2\gamma}gt\right)^2 - \frac{2g}{\gamma}x}, & x \leq c_0 t - \frac{g}{2}t^2. \end{cases} \quad (16)$$

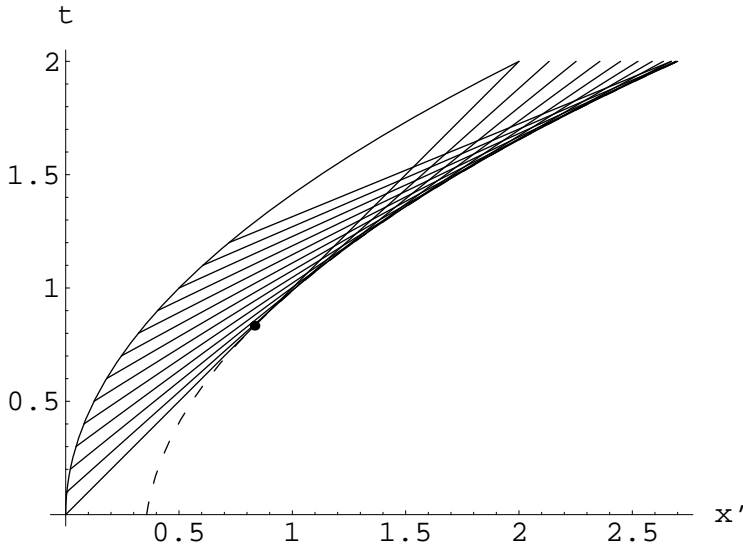


Figure 1: Line described by the ground and forward characteristics in the falling frame (in units such that $c_0 = g = 1$ and for $\gamma = 7/5$). The dashed line $(\partial x'/\partial v')_t = 0$ is the envelope of the characteristic lines. At the cusp point $(5/6, 5/6)$, the characteristics cross and the solution becomes multivalued.

For a simple wave, the density is a definite function of the velocity [2]. We can calculate it from Eq. (5) to be

$$\rho(x, t) = \rho_0 \left[1 + \frac{\gamma - 1}{2} \frac{v(x, t) + gt}{c_0} \right]^{\frac{2}{\gamma - 1}}. \quad (17)$$

These expressions for ρ and v constitute the solution of Eqs. (7) and (12) with the given boundary conditions.

We note a peculiarity of the solution found above: the wave front's coordinate $x_f = c_0 t - gt^2/2$ begins increasing but, for $t > c_0/g$, turns to decreasing and, eventually, returns to the origin (a free fall with initial velocity c_0). On the other hand, a shock wave singularity occurs before the turning point: One can calculate $(\partial x/\partial v)_t$, and its null locus defines a line in the xt -plane, namely, $x = [2c_0 + (\gamma - 1)gt]^2/(8\gamma g)$. Initially, the corresponding x is larger than x_f , so it is unphysical, but, for $t = 2c_0/[(\gamma + 1)g]$, it meets the wave front; that is, the falling gas overtakes the gas just below it and a shock wave arises. The relevant geometry is represented in Fig. 1, in the falling reference frame. From the moment of formation of the shock onwards, the solution (16,17) ceases to be valid. Furthermore, the analysis of the propagation of a shock wave cannot be done in terms of simple waves.

4 Similarity solution with constant gravity

When the initial conditions are sufficiently simple, the solution of a one-dimensional gas flow problem may adopt a self-similar structure and be greatly simplified by writing the

equations in the appropriate variables [2, 6], in which the partial differential equations become ordinary differential equations (ODE).

In our case, a self-similar solution is not possible, since we have too many parameters in the initial conditions. Nevertheless, it is commonly observed that nonlinear equations that do not have similarity solutions at the outset develop them in an *intermediate asymptotic* regime, that is, a regime between two very different scales where both scales can be neglected [7]. We shall see that we can find a similarity solution of this kind.

In the equations with constant gravity, namely, (3), (4) and (12), R and GM only appear in the combination $g = GM/R^2$; furthermore, the only parameter in the initial and boundary conditions is ρ_0 . Hence, we have one less parameter. However, we can still form the two *independent* dimensionless variables gt/c_0 and gx/c_0^2 , so we will have to remove another parameter to have a similarity solution.

If we assume that the initial gas temperature is very low, then $c_0 \rightarrow 0$ and the only independent dimensionless variable is $\xi = x/(gt^2)$ (we measure the distance x from the ground). This corresponds to the intermediate asymptotics $c_0^2/g \ll x \ll R$; equivalently, in terms of the dimensionless height variable $x^* = gx/c_0^2$, it corresponds to $1 \ll x^* \ll R^* = \mathcal{R}/R$ (recall that $\mathcal{R} \gg R$).

To take into account the presence of shock waves and the consequent dissipation, we consider the full set of equations (3), (4) and (12). We can express them in dimensionless form by introducing new variables:

$$v = \frac{x}{t}u, \quad \rho = \rho_0 r, \quad P = \frac{x^2}{t^2} \rho_0 p. \quad (18)$$

Some straightforward algebra then yields,

$$\xi[u' + (u - 2)\frac{r'}{r}] + u = 0, \quad (19)$$

$$(u - 2)\xi u' + u^2 - u = -\xi^{-1} - r^{-1}(2p + \xi p'), \quad (20)$$

$$(u - 2)\xi[\ln(p/r^\gamma)]' + 2(u - 1) = 0. \quad (21)$$

Upon making the change of variables

$$\begin{cases} \xi = \tilde{\xi} - \frac{1}{2}, \\ u = \frac{\tilde{\xi}\tilde{u} - 1}{\tilde{\xi}}, \\ p = \frac{\tilde{\xi}^2\tilde{p}}{\tilde{\xi}^2} \end{cases} \quad (22)$$

(corresponding to changing to the falling reference frame), the ξ^{-1} term in the second equation vanishes and the system of ordinary differential equations simplifies to

$$\tilde{\xi}[\tilde{u}' + (\tilde{u} - 2)\frac{r'}{r}] + \tilde{u} = 0, \quad (23)$$

$$(\tilde{u} - 2)\tilde{\xi}\tilde{u}' + \tilde{u}^2 - \tilde{u} = -r^{-1}(2\tilde{p} + \tilde{\xi}\tilde{p}'), \quad (24)$$

$$(\tilde{u} - 2)\tilde{\xi}[\ln(\tilde{p}/r^\gamma)]' + 2(\tilde{u} - 1) = 0. \quad (25)$$

Similarity equations of this type have also been studied in Ref. [4]. However, the authors do not make the change to the falling reference frame, and restrict themselves to solving the equations by a series expansion near the ground. Instead, we follow here the general methods exposed in Ref. [6].

In terms of the variable $\tau = \ln \tilde{\xi}$, the previous equations imply a system of autonomous nonlinear ODE, namely,

$$\frac{d\tilde{u}}{d\tau} = \frac{\tilde{p}(\tau) [2 + \gamma \tilde{u}(\tau)] - r(\tau) \tilde{u}(\tau) (2 - 3 \tilde{u}(\tau) + \tilde{u}(\tau)^2)}{-\gamma \tilde{p}(\tau) + r(\tau) [\tilde{u}(\tau) - 2]^2}, \quad (26)$$

$$\frac{dr}{d\tau} = r(\tau) \frac{-2 \tilde{p}(\tau) + r(\tau) [\tilde{u}(\tau) - 2] \tilde{u}(\tau)}{(-\gamma \tilde{p}(\tau) + r(\tau) [\tilde{u}(\tau) - 2]^2) [\tilde{u}(\tau) - 2]}, \quad (27)$$

$$\frac{d\tilde{p}}{d\tau} = \tilde{p}(\tau) \frac{2 \gamma \tilde{p}(\tau) - r(\tau) (4 - (6 + \gamma) \tilde{u}(\tau) + 2 \tilde{u}(\tau)^2)}{-\gamma \tilde{p}(\tau) + r(\tau) [\tilde{u}(\tau) - 2]^2}. \quad (28)$$

Given the homogeneity properties of these equations with respect to \tilde{p} and r , it proves convenient to introduce the variable $\theta = \tilde{p}/r$ (the dimensionless form of the temperature for the perfect gas with pressure P and density ρ). Thus,

$$\frac{d\theta}{d\tilde{u}} = \theta \frac{2 \theta (1 + \gamma (\tilde{u} - 2)) - (\tilde{u} - 2) (4 - (5 + \gamma) \tilde{u} + 2 \tilde{u}^2)}{(\tilde{u} - 2) (\theta (2 + \gamma \tilde{u}) - \tilde{u} (2 - 3 \tilde{u} + \tilde{u}^2))} \quad (29)$$

The solution of this equation provides the relation between the “velocity” \tilde{u} and the “temperature” θ , $\theta(\tilde{u})$. Substituting it back into Eq. (26), we have an ODE for $\tilde{u}(\tau)$, which is immediately solved by a quadrature. Analogously, one solves for $r(\tau)$.

We must now translate the initial and boundary conditions of the original partial differential equations (PDE) into an initial condition for the ODE (29): at $t = 0$, $\rho(0, x) = \rho_0$, $P(0, x) = P_0 = 0$ ($c_0 \rightarrow 0$), and $v(0, x) = 0$, implying that $r = 1$ and $u = 0$ for $\tilde{\xi} = \xi = \infty$; at $x = 0$, $v = 0$, which implies, since $v = gt(\tilde{\xi}\tilde{u} - 1)$, that $\tilde{u} = 2$ for $\xi = 0$ and $\tilde{\xi} = 1/2$. The problem seems overdetermined. However, recalling the exact solution of section 3, which gives rise to a discontinuity (shock wave), we expect that the self-similar solution is discontinuous, so that there is no contradiction (in fact, this happens in most self-similar solutions [2, 6]).

When discontinuities arise, the original differential equations break down, but they can be expressed as integrals over test functions, which may have discontinuous solutions (*weak solutions*) [1, 2, 3]. Integration of Eq. (11) across a discontinuity yields the Rankine-Hugoniot jump conditions $\mathbf{F}(\mathbf{U}_1) = \mathbf{F}(\mathbf{U}_2)$. These conditions can be written as

$$\begin{cases} \rho_1 v_1 = \rho_2 v_2, \\ \rho_1 v_1^2 + P_1 = \rho_2 v_2^2 + P_2, \\ \frac{v_1^2}{2} + \frac{P_1}{\rho_1} + e_1 = \frac{v_2^2}{2} + \frac{P_2}{\rho_2} + e_2, \end{cases} \quad (30)$$

where subscripts refer to the values on each side of the shock and e is the internal energy; for a perfect gas, $e = P/[\rho(\gamma - 1)]$. These equations hold in a coordinate system in which

the shock surface is at rest. On the other hand, the location of the shock must be at fixed ξ , say ξ_s (the subscript s will denote variables pertaining to the shock motion). Consequently, the shock wave velocity is

$$v_s = \frac{dx_s}{dt} = \xi_s g \frac{dt^2}{dt} = 2\xi_s g t = 2 \frac{x_s}{t},$$

that is, $u_s = 2$ (and also $\tilde{u}_s = 2$). Then,

$$\begin{cases} r_1(u_1 - 2) = r_2(u_2 - 2), \\ p_1 + r_1(u_1 - 2)^2 = p_2 + r_2(u_2 - 2)^2, \\ \frac{(u_1 - 2)^2}{2} + \frac{\gamma}{\gamma - 1} \frac{p_1}{r_1} = \frac{(u_2 - 2)^2}{2} + \frac{\gamma}{\gamma - 1} \frac{p_2}{r_2}, \end{cases} \quad (31)$$

valid in both the rest and the falling reference frames. Using the falling frame and eliminating r_2/r_1 between the first and second equations,

$$\begin{cases} \frac{\theta_1}{\tilde{u}_1 - 2} + \tilde{u}_1 - 2 = \frac{\theta_2}{\tilde{u}_2 - 2} + \tilde{u}_2 - 2, \\ (\tilde{u}_1 - 2)^2 + \frac{2\gamma}{\gamma - 1} \theta_1 = (\tilde{u}_2 - 2)^2 + \frac{2\gamma}{\gamma - 1} \theta_2. \end{cases} \quad (32)$$

We have obtained an involutive mapping of the plane (\tilde{u}, θ) as the relation between the variables at either side of the shock discontinuity. Since we have the condition that as $x \rightarrow \infty$ we go to $(0, 0)$ and (in the falling frame) these values hold all the way down to the shock surface, we just need the image of the origin under the mapping. This yields the point $(4/(\gamma + 1), 8(\gamma - 1)/(\gamma + 1)^2)$. Therefore, we need the solution of Eq. (29) that goes through this point. We can see in the example of Fig. 2 ($\gamma = 7/5$) that the strand of this solution that departs from $(5/3, 5/9)$ ends at the point $(2, 0)$, hence satisfying the boundary condition at $x = 0$.¹

Now, substituting the function just computed back into Eq. (26), we obtain

$$d\tau = \frac{\gamma \theta(\tilde{u}) - (\tilde{u} - 2)^2}{-\theta(\tilde{u}) (2 + \gamma \tilde{u}) + \tilde{u} (2 - 3\tilde{u} + \tilde{u}^2)} d\tilde{u}, \quad (33)$$

from which we can deduce the interval of τ between the points $(4/(\gamma + 1), 8(\gamma - 1)/(\gamma + 1)^2)$ and $(2, 0)$ by integration. The result for $\gamma = 7/5$ is 0.0880104. Hence, we obtain the quotient between the corresponding values of ξ . This quotient gives the location of the shock relative to the ground: $\tilde{\xi}_s/(1/2) = \exp 0.0880104 = 1.09200 \Rightarrow \xi_s = 0.0919995/2 = 0.0459997$, so that the coordinate of the shock is $x_s = 0.0459997gt^2$.

Once we have described the self-similar solution, let us analyze in detail its range of validity. The self-similar solution is valid for $c_0 \rightarrow 0$, that is, for the dimensionless variables $t^* = gt/c_0$ and $x^* = gx/c_0^2$ sufficiently large. Moreover, $x^* \ll R^*$, but the upper limit of the t^* asymptotics is still indefinite. The remaining condition can be found by using the

¹Notice that this implies that the asymptotics $c_0 \rightarrow 0$ is of the *first kind* (the simple case) according to the denomination of Barenblatt [7].

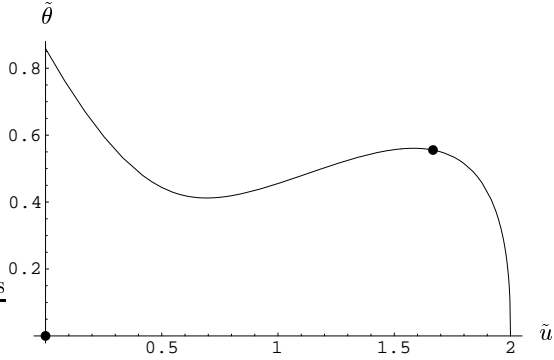


Figure 2: Relevant solution of the ODE (29) for $\gamma = 7/5$, displaying the origin and its image at the shock surface, the point $(5/3, 5/9)$.

dimensionless variables $\xi = x^*/(t^*)^2 = x/(gt^2)$ and $\zeta = x^*/t^* = x/(c_0 t)$, such that the former only depends on g and the latter on c_0 . We have that $c_0 \rightarrow 0$ implies that $\zeta \gg 1$. To realize the consequences of the previous conditions it is convenient to consider the logarithmic variables $\ln x^*$ and $\ln t^*$, on the one hand, and the linearly related variables $\ln \xi$ and $\ln \zeta$, on the other hand. The three equations $\ln x^* = \ln R^*$, $\ln t^* = 0$ and $\ln \zeta = 0$ define a triangle in the $(\ln x^*, \ln t^*)$ plane in which the complete intermediate asymptotics holds; to be precise, in the interior region far from the borders. Moreover, part of this region corresponds to the trivial solution above the shock (the part with $\xi > \xi_s$).

5 Similarity solution with variable gravity

For heights of the order of the ball radius or larger, we have to return to the full continuity equation (2) and reset $g(x) = GM/(x + R)^2$ in the Euler equation (3). We have an additional parameter, namely, the radius R . If we further assume that $R \rightarrow 0$, we can find a similarity solution, that is, in the intermediate asymptotics $R \ll x \ll \mathcal{R}$ ($R^* \ll x^* \ll (R^*)^2$). Now, the dimensionless variable ξ becomes $\xi = x^3/(GMt^2)$. Hence, we can express the continuity and Euler equations as

$$\xi[3u' + (3u - 2)\frac{r'}{r}] + 3u = 0, \quad (34)$$

$$(3u - 2)\xi u' + u^2 - u = -\xi^{-1} - r^{-1}(2p + 3\xi p'). \quad (35)$$

The energy equation becomes

$$(3u - 2)\xi[\ln(p/r^\gamma)]' + 2(u - 1) = 0. \quad (36)$$

These three equations look similar to the ones corresponding to constant gravity, but they are more difficult to analyze:² the change of variables that transformed the latter into

²An extensive study of self-similar spherical accretion with an initial power-law density distribution is provided by Ref. [5].

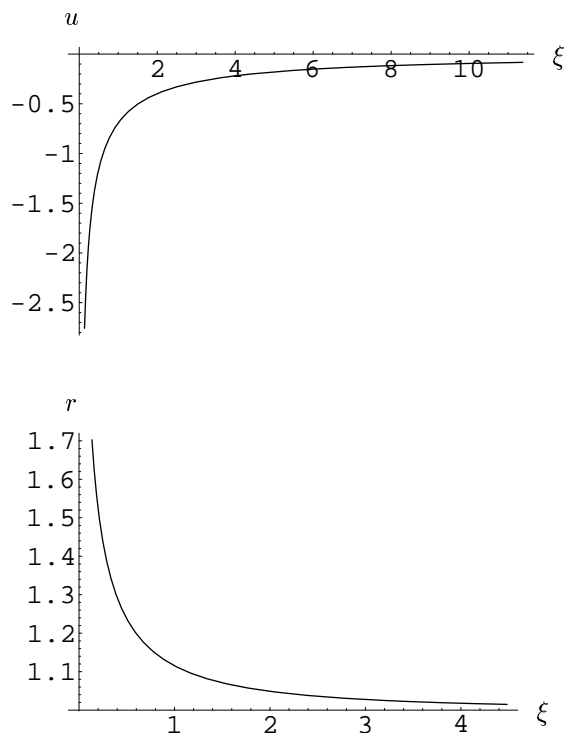


Figure 3: Similarity solution $\{u(\xi), r(\xi)\}$ for free fall with varying gravity.

an autonomous system is not available. In fact, the free-fall (pressureless) problem is now nontrivial, but it can be solved (see Appendix). The solution, in parametric form, reads

$$\xi = \frac{8 \cos^6 \alpha}{2\alpha + \sin(2\alpha)}, \quad (37)$$

$$u = -\left(\alpha + \frac{\sin(2\alpha)}{2}\right) \frac{\sin \alpha}{\cos^3 \alpha}, \quad (38)$$

$$r = \frac{\rho}{\rho_0} = \frac{8 \cos^{-3} \alpha}{9 \cos \alpha - \cos(3\alpha) + 12 \alpha \sin \alpha}, \quad (39)$$

where $\alpha \in (0, \pi/2)$. The corresponding graphs for u and r are shown in Fig. 3.

As regards the complete similarity solution, it must match the free fall solution outside a spherical shock wave with the inner solution with pressure. In turn, this solution should be matched with the previous solution near the ground. These matchings are difficult to obtain analytically, so we will rather rely on numerical solutions (next section). At any rate, we deduce that, as the shock moves from $x_s \ll R$ to $x_s \gg R$, its velocity experiences a crossover from $v_s = 2x_s/t = 2\xi_s g t$ to $v_s = 2/3(x_s/t) = 2/3(GM\xi_s)^{1/3} t^{-1/3}$ (with *different* ξ_s), changing from accelerating to decelerating. In addition, the shock must disappear when $t \gg GM/c_0^3$ and $x_s \gg \mathcal{R}$ (see section 7).

Of course, a rough analysis of the range of validity of this similarity solution is also possible. It is valid for $R \rightarrow 0$, that is, for the dimensionless variables $\hat{x} = x/R$ and $\hat{t} = \sqrt{GM}/R^{3/2} t$ sufficiently large. It is convenient to use the dimensionless variables

$\xi = \hat{x}^3/\hat{t}^2$ and $\zeta = \hat{x}/\hat{t} = \sqrt{R/GM} x/t$, such that the former does not depend on R . We have that $R \rightarrow 0$ implies that $\zeta \ll 1$. Considering the logarithmic variables $\ln \hat{x}$ and $\ln \hat{t}$, on the one hand, and the linearly related variables $\ln \xi$ and $\ln \zeta$, on the other hand, the three equations $\ln \hat{x} = 0$, $\ln \hat{t} = 3/2 \ln(\mathcal{R}/R)$ and $\ln \zeta = 0$ define the triangle wherein the complete intermediate asymptotics holds (far from the borders).

6 Numerical solution

In this section we will numerically validate and complement the main results obtained above. As was mentioned in section 2, our aim is to integrate the equation

$$\frac{\partial \mathbf{U}}{\partial t} + \frac{\partial \mathbf{F}(\mathbf{U})}{\partial x} = \mathbf{G}(\mathbf{U}) \quad (40)$$

for the cases of constant and varying gravity. Relying on the operator splitting approach, we integrate first the conservative part of the equation using the Lax numerical scheme and then integrate the source term:

$$\mathbf{U}_j^{n+1} = \frac{\mathbf{U}_{j+1}^n + \mathbf{U}_{j-1}^n}{2} - \Delta t \frac{\mathbf{F}(\mathbf{U}_{j+1}^n) - \mathbf{F}(\mathbf{U}_{j-1}^n)}{2 \Delta x} + \Delta t \mathbf{G}(\mathbf{U}_j^n). \quad (41)$$

With this we get a discrete approximation of the value of \mathbf{U} at $x_j = j\Delta x$ and time $t = n\Delta t$ to second order accuracy, \mathbf{U}_j^n . We will show the results in dimensionless variables $x^* = x/(c_0^2/g)$ and $t^* = t/(c_0/g)$ and fix $\Delta x^* = 0.005$ and $\Delta t^* = \frac{\Delta x^*}{20}$. We have chosen Δt so that the Courant-Friedrichs-Lewy stability condition of the scheme is satisfied [8]. This condition essentially states that we are required to choose a time step smaller than the smallest characteristic physical time in the problem, $\Delta t^* \leq \frac{\Delta x^*}{|v_{max}^*|}$, which is the time for the velocity to lead to a flow over a distance Δx^* (during our integration time $v^* = v/c_0 \leq v_{max}^* = 20$). We integrate the problem with initial condition $\rho(x, 0) = 1$, $P(x, 0) = \gamma c_0^2 \rho_0$, $v(x, 0) = 0$, adiabatic index $\gamma = 7/5 = 1.4$ and boundary condition at the solid surface $v(t, 0) = 0$.

In the case of constant gravity, we can rewrite the equations of gas downfall on a flat surface (7) and (12) in the divergence form (40) using $\mathbf{G}(\mathbf{U}) = (0, -g\rho, -g\rho v)$ (as was mentioned in section 3). We show in Fig. 4 (left) the density evolution in (decimal) logarithmic scale for the case of constant gravity. For the initial stages up to $t^* = \frac{2}{\gamma+1} \approx 0.83$, before the shock wave develops, the density and velocity values are coincident with those given by the analytical solutions Eqs. (16) and (17) (section 3). Then the shock formation induces a discontinuity in the density, pressure and velocity distribution and the analytic solution is no longer valid. For a polytropic gas and based on the Rankine-Hugoniot conservation conditions across the shock, one can see that the ratios v_2/v_1 and P_2/P_1 can be arbitrarily large, whereas (for these strong shocks) when $P_2/P_1 \rightarrow \infty$, the density ratio ρ_2/ρ_1 tends to the constant limit $\rho_2/\rho_1 = (\gamma + 1)/(\gamma - 1)$ [2]. In our case with g constant, the pressure and velocity variation across the shock continue to grow as long as the shock exists, while the discontinuity in the density tends to the limiting value $\rho_2/\rho_1 = 6$ ($\gamma = 1.4$), as is shown in the lateral view of the density in Fig. 4 (right).

Following the asymptotic similarity analysis we expect the shock position x_s to move as $x_s \approx \xi_s g t^2$, for the case of constant gravity (section 4), or equivalently $x_s^* = \xi_s (t^*)^2$. In Fig. 5 (left) we plot all the points x^* , in the area affected by the wave ($x^* | \rho(x^*, t^*) > \rho_0$) rescaled by $(t^*)^2$. The shock front is at the upper limit of this area. The value $\xi = x_s^*/(t^*)^2$ (evaluated at the shock) evolves to a constant value $\xi_s = 0.046$ and therefore, beyond a transient time, the shock moves with constant acceleration. This is in agreement with the analytic prediction.

Next we study the time evolution of this process with spherical symmetry for the case of varying gravity, with $\mathbf{G}(\mathbf{U}) = (-2\rho v/(x+R), -2\rho v^2/(x+R) - g(x)\rho, -2(\rho e + \rho v^2/2 + P)/(x+R) - g(x)\rho v)$, $g(x) = gR^2/(x+R)^2$ and g the gravity at the surface of the ball. For our study case we choose $R^* = R/(c_0^2/g) = 10$. We restrict ourselves to this relatively small value because the magnitude of the discontinuity at the shock and the velocity of the downfalling gas increase with R^* . So the spatial and temporal grid sizes must be fixed sufficiently small to be able to handle these sharp discontinuities and satisfy the Courant-Lewy condition for maximal velocities in the grid. This in turn imposes a limitation on the maximal R^* to be considered.

We remark that, of course, the numerical integration has to be restricted to a finite interval of x^* , namely $[0, x_{max}^*]$, and therefore we need a boundary condition at x_{max}^* . This is not a problem in the constant g case, because what happens for large x^* is *exactly* known: the gas is in free fall with acceleration g and $\rho = \rho_0$ (this is a valid boundary condition as long as the shock front has not reached x_{max}^*). In contrast, in the varying $g(x)$ case, we impose as boundary condition the initial values $\rho(t, x_{max}^*) = \rho_0$ and $P(t, x_{max}^*) = P_0 = \gamma c_0^2 \rho_0$, which are similar to the real values if $x_{max}^* \gg (R^*)^2$ and as long as the shock front is sufficiently far from x_{max}^* . For our calculations we use $x_{max}^* = 450$.

In Fig. 5 (right) we plot x^*/t^* vs. t^* in (natural) logarithmic scale. The lower area is the area between the shock front and the surface. As one can see in the Figure, we can fit the motion of the shock front as $x_s^*/t^* = (t^*)^{-1/3} \exp(-0.72)$. We get the corresponding value of $\xi_s = \frac{(x_s^*)^3}{(t^*)^2 (R^*)^2} = 0.0011$. Over this short range of distances and time, we are already able to find the asymptotic behaviour predicted in section 5 in spite of the strong conditions needed for the derivation of the similarity solution $c_0 \rightarrow 0$ and $R \rightarrow 0$ which are hardly satisfied in this particular case (for these cases v is not so large as compared to c_0 , see Fig. 6 for a more detailed view of the dynamics of the main physical quantities).

7 Transition to the static state

The dissipation associated with the shock wave makes us expect that the gas must reach a stationary state with more entropy than the initial state. The properties of the stationary state are easily studied through the hydrostatic equation,

$$\int \frac{dP}{\rho} = - \int g dx,$$

with $P \propto \rho^\gamma$ and with either constant or variable gravity $g(x) = GM/(x+R)^2$. It is easy to obtain the solution in the latter case (the constant g solution can be obtained expanding

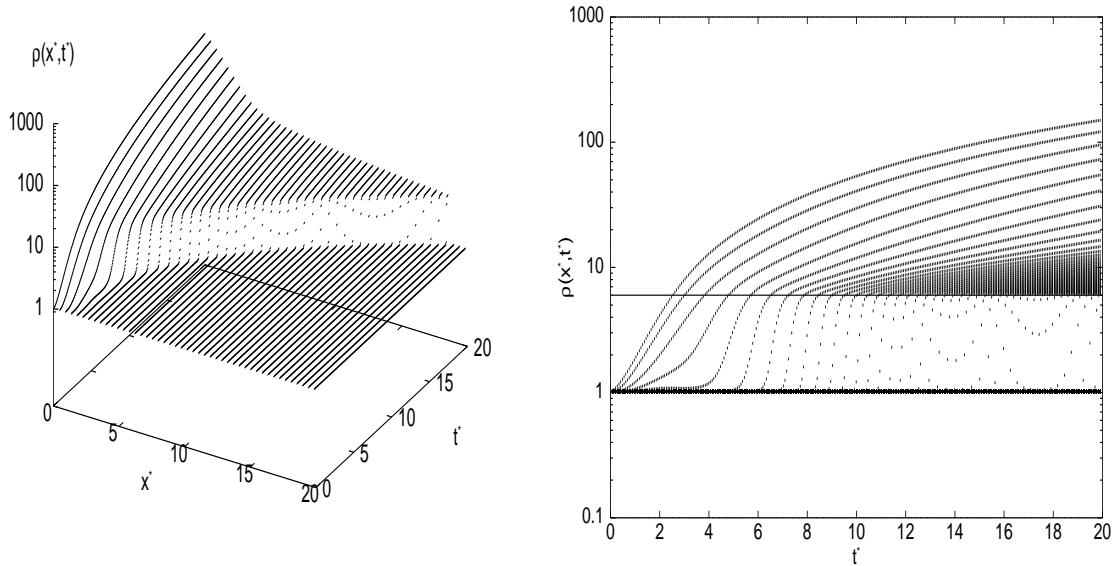


Figure 4: Density distribution and time evolution (for constant g) in (decimal) logarithmic scale. Three-dimensional view (left) and lateral view (right). The density ratio across the shock tends to $\rho_2/\rho_1 = (\gamma + 1)/(\gamma - 1) = 6$ as expected for a polytropic gas.

this solution in x/R or directly):

$$\left(\frac{\rho}{\rho_b}\right)^{\gamma-1} = 1 - \frac{\gamma-1}{\gamma} \frac{\rho_b g_b R}{P_b} \left(1 - \frac{R}{x+R}\right), \quad (42)$$

where the subscript b denotes values at the ball's surface. It is more convenient to take the reference at infinity, where the density and pressure keep their initial values, so that

$$\left(\frac{\rho}{\rho_0}\right)^{\gamma-1} = 1 + \frac{\gamma-1}{\gamma} \frac{\rho_0}{P_0} \frac{GM}{x+R} = 1 + (\gamma-1) \frac{\mathcal{R}}{x+R}. \quad (43)$$

The transition to the static state is best studied numerically. Next we show, for the case of varying gravity with $R^* = 7$, two snapshots of the spatial distribution of the main physical quantities ($v^* = v/c_0$, the speed of sound in the media $c^* = c/c_0 = \sqrt{P^*\gamma/\rho}$ with $P^* = P/c_0^2$, and ρ/ρ_0) as obtained from the numerical integration explained in section 6, compared with the values of the static solution given by equation (43). In Fig. 6 (left), we observe that the shock front appears as a discontinuity of the main variables when the speed of the downfalling gas is greater than the speed of sound (supersonic regime). The shock discontinuity decreases in magnitude once the gas speed v^* is no longer supersonic. In Fig. 6 (right) we can see how the numerical solution tends to the static solution. As the shock moves away the gas behind slows down and finally becomes still.

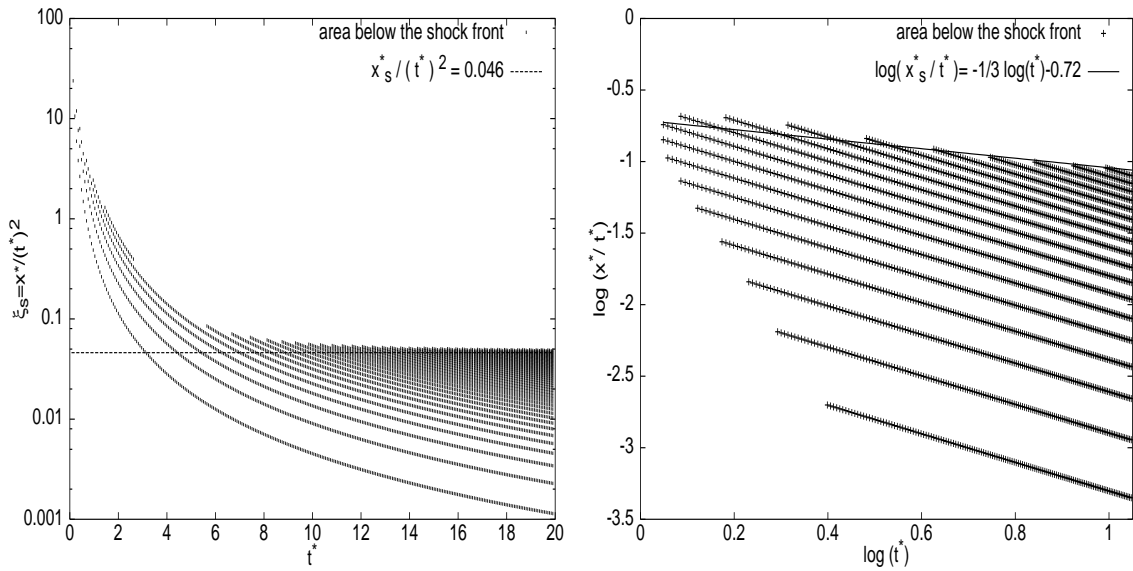


Figure 5: Self-similar evolution. We plot, for all the points x^* between the surface and the shock front, the time evolution of: (left) $\xi = x^*/(t^*)^2$ for the case of constant gravity and (right) (x^*/t^*) in logarithmic scale for the case of varying gravity with $R^* = 10$. (Left) If gravity does not change with height, the value of ξ at the shock front (upper line) tends to a constant value $\xi_s = 0.046$. (Right) When gravity changes with height, at the shock front (upper line) we can fit $x_s^*/t^* = (t^*)^{-1/3} \exp(-0.72)$ and therefore $\xi_s = \frac{(x_s^*)^3}{(t^*)^2 (R^*)^2} = 0.0011$. Both results are in agreement with the analytic predictions of self-similar solutions.

8 Discussion

Summarizing, we have divided the space dimension (the radial distance x) into a near zone (near the ball's surface, where $x \ll R$) and a far zone ($x \gg R$). In the near zone, we have obtained an exact solution for short time and a self-similar regime for longer time and radius. In the far zone, we have a self-similar regime for relatively long time and radius. The parameter controlling the extent of both intermediate asymptotic regimes is $R^* = \mathcal{R}/R$. We have also obtained an exact static state for very long times. Even though the regions of validity of the analytic solutions occupy a small part of the plane (x, t) , the numerical study provides an interpolation between them, in addition to verifying those solutions. Therefore, the combined solutions provide a good intuitive understanding of the entire dynamics. The crucial feature is the formation and propagation of a shock wave until its dissipation.

We have integrated numerically the equations of this dynamical system with a robust scheme that, respecting the flux conservative structure of the equations, is able to reproduce the dynamics in the neighbourhood of the shock front. We observe that as soon as the gas velocity is above the speed of sound in the media a sharp discontinuity appears in all the relevant variables. In the case of constant gravity the magnitude of this discontinuity increases up to a constant value whereas the pressure and velocity increase indefinitely. In

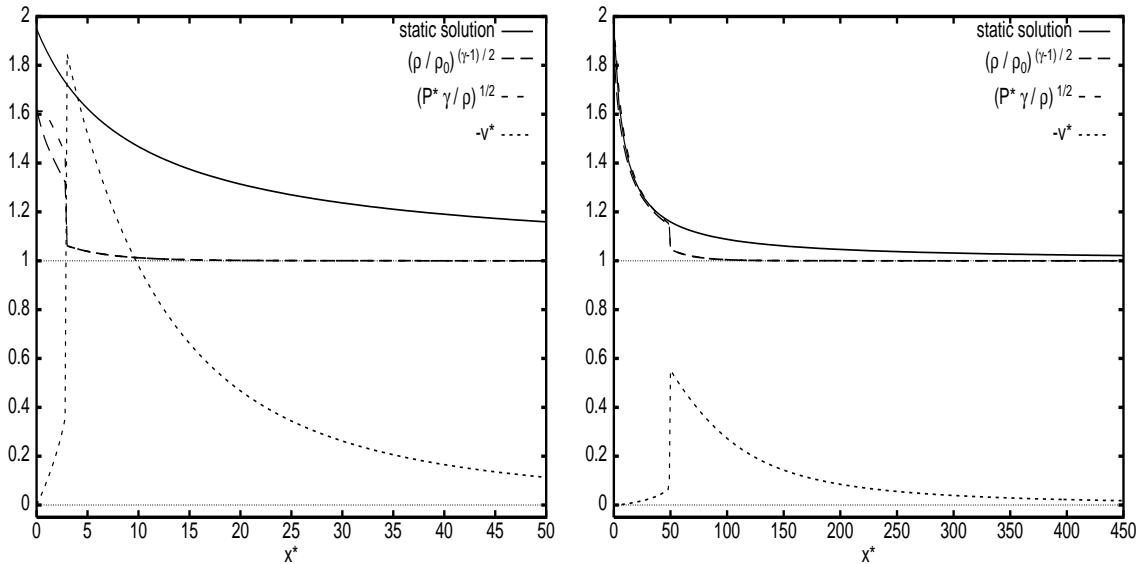


Figure 6: Simulations for $R^* = 7$: (Left) At $t^* = 6$, in a certain range of x^* , the speed of the downfalling gas v^* is greater than the speed of sound in the media $c^* = \sqrt{P^* \gamma / \rho}$ and a shock front is formed. At this discontinuity the gas is no longer polytropic and $P^* \gamma / \rho$ is not given by $(\rho / \rho_0)^{\gamma-1}$. For comparison we include the asymptotic solution or static solution given by equation (43). (Right) At $t^* = 70$ the speed is not supersonic, and the gas is polytropic again. As the front moves away from the ball surface, the density and pressure tend to the static solution.

the case of varying gravity, the highest discontinuities are reached in the region $x_s \ll \mathcal{R}$, then the shock front moves away from the ball and the magnitude of the discontinuity decreases. It is interesting as well to remark that the shock wave is particularly robust and holds for $x_s > \mathcal{R}$ (see the sharp discontinuity in Fig. 6 (right)).

Since the propagation of the shock wave mostly takes place in the regimes with negligible P_0 (if $R^* \gg 1$), it is interesting to consider the one-dimensional fluid dynamics equations for pressureless gas, namely, the Burgers equation for the velocity (plus the continuity equation, independent of it). The Burgers equation includes viscosity ν , but in the limit of vanishing viscosity its only effect is to prevent the velocity from becoming multi-valued, giving rise to shocks [9]. Furthermore, the formation of shocks can be determined analytically for *any* initial condition. Therefore, it seems that the intermediate asymptotic regimes should be given by the corresponding exact solution of the Burgers equation, which is trivial: the gas is in free fall everywhere but the velocity is discontinuous at the ball's surface, in order that it be zero on it. In other words, the shock is always at the ball's surface and does not propagate. This corresponds to the pressureless *dust* being deposited on the surface, where the density becomes infinite but immediately jumps to its free-fall value. Hence, we can appreciate the importance of the dissipation associated to the shock wave: whereas in the Burgers equation the kinetic energy of the free-falling dust is simply ignored after it inelastically collides with the ground, in the real intermediate asymptotic

solutions it serves to heat the gas below the shock wave, producing pressure where there was none. This dissipation is connected with the breakdown of the thermodynamic equation (4), which, in the case that this equation expresses entropy conservation, indicates that entropy is created at the shock. The sharp rise of temperature and pressure behind the shock are clearly visible in the numerical simulations.

Acknowledgments

We thank F. Barbero, A. Domínguez, R. Gómez-Blanco, A. Mancho and J. Pérez-Mercader for conversations and comments. Furthermore, we thank the two referees of this paper for advise that has greatly contributed to improve it. The work of J. Gaité is supported by a “Ramón y Cajal” contract and by grant BFM2002-01014, both of the Ministerio de Ciencia y Tecnología. M.-P. Zorzano acknowledges an INTA fellowship for training in astrobiology.

Appendix: Similarity solution for the free fall in the field of a point-like mass

We describe here the “Lagrangian solution” of Eq. (35) with $p = 0$, that is,

$$(3u - 2) \xi u' + u^2 - u = -\xi^{-1}. \quad (44)$$

Since the initial condition is given at $\xi \rightarrow \infty$, it is convenient to make the change of variable $\hat{\xi} = \xi^{-1}$, transforming the equation into

$$\frac{du}{d\hat{\xi}} = \frac{u^2 - u + \hat{\xi}}{(3u - 2)\hat{\xi}}. \quad (45)$$

The point (0,0) is a singular point of the ODE. Its solution is unspecified, unless we introduce an additional condition. The initial condition $v = 0$ implies that $v = \sqrt{\frac{GM}{x}} \hat{\xi}^{-1/2} u$ goes to zero as $\hat{\xi} \rightarrow 0$. To impose it, it is best to linearize and solve the ODE around (0,0): The general solution of

$$\frac{du}{d\hat{\xi}} = \frac{-u + \hat{\xi}}{-2\hat{\xi}} \quad (46)$$

is $u = -\hat{\xi} + C \sqrt{\hat{\xi}}$, so that the singular point is a node. Then, $\lim_{\hat{\xi} \rightarrow 0} \hat{\xi}^{-1/2} u = C$. Hence, the particular solution of the nonlinear equation (45) in which we are interested is the only one that satisfies $u'(0) = -1$.

In the Lagrangian picture, the velocity is given by energy conservation as

$$v = -\sqrt{2\left(E + \frac{GM}{x}\right)}. \quad (47)$$

The initial condition that the particle is at rest implies that $E = -GM/x_0$. Hence,

$$u = \frac{t}{x} v = -\sqrt{2\xi^{-1}\left(1 - \frac{x}{x_0}\right)}, \quad (48)$$

and to have a self-similar form we must express x/x_0 as a function of ξ . In order to do it, we must solve the equation of motion (47):

$$t = - \int_{x_0}^x \frac{ds}{\sqrt{2(GM/s - GM/x_0)}} = - \frac{x_0^{3/2}}{\sqrt{GM}} \int_1^{x/x_0} \frac{d\sigma}{\sqrt{2(1/\sigma - 1)}}, \quad (49)$$

where we have introduced $\sigma = s/x_0$ to write it in a self-similar form. It is clear now that $\xi^{-1/2} = F(x/x_0)$, which can be inverted to obtain x/x_0 as a function of ξ . The substitution of this function in Eq. (48) yields the solution of the ODE that satisfies the appropriate initial condition.

One can calculate the integral in Eq. (49) by the change of variables $\sigma = \cos^2 \varphi$. This allows one to obtain the solution of the differential equation (44) in parametric form: Let

$$\cos^2 \alpha = x/x_0; \quad (50)$$

then,

$$\frac{\sqrt{GM} t}{x_0^{3/2}} = \frac{1}{\sqrt{2}} \left(\alpha + \frac{\sin(2\alpha)}{2} \right), \quad (51)$$

and

$$\xi^{-1/2} = \frac{1}{\sqrt{2}} \cos^{-3}(\alpha) \left(\alpha + \frac{\sin(2\alpha)}{2} \right), \quad (52)$$

$$u = - \cos^{-3}(\alpha) \left(\alpha + \frac{\sin(2\alpha)}{2} \right) \sin \alpha, \quad (53)$$

where $\alpha \in (0, \pi/2)$. It is easy to verify that this parametric solution fulfills the initial condition $\lim_{\xi \rightarrow \infty} u' = -1$.

In the Lagrangian formulation, the density is given by

$$\rho = \left(\frac{\partial x_0}{\partial x} \right)_t \frac{x_0^2}{x^2} \rho_0,$$

where x_0^2/x^2 is a spherical geometry factor. From Eqs. (50), (51) and (52),

$$r = \frac{\rho}{\rho_0} = \frac{8 \cos^{-3}(\alpha)}{9 \cos(\alpha) - \cos(3\alpha) + 12 \alpha \sin(\alpha)}, \quad (54)$$

which, together with Eq. (52), constitute the parametric equations of the density.

References

- [1] R. Courant and K.O. Friedrichs, *Supersonic Flow and Shock Waves*, New York, Interscience Publishers, 1948
- [2] L.D. Landau and E.M. Lifshitz, *Fluid Mechanics*, Pergamon Press, Oxford (1987)

- [3] A.J. Chorin and J.E. Marsden, *A Mathematical Introduction to Fluid Mechanics*, TAM 4, 3rd edition, Springer-Verlag, NY (1993)
- [4] G.S. Bisnovaty-Kogan, Ya.B. Zel'dovich and D.K. Nadezhin, *Soviet Astronomy* **16**, 393 (1972)
- [5] Ya.M. Kazhdan and M. Murzina, *Mon. Not. R. Astron. Soc.* **270**, 351–363 (1994)
- [6] L.I. Sedov, *Similarity and Dimensional Methods in Mechanics*, MIR, Moscow (1982)
- [7] G.I. Barenblatt, *Scaling, Self-Similarity, and Intermediate Asymptotics*, Cambridge University Press (1996)
- [8] R. D. Richtmyer and K. W. Morton, *Difference Methods for Initial-Value Problems*, Interscience Publishers, John Wiley & Sons (1967)
- [9] E. Hopf, *Comm. Pure Appl. Math.* **3**, 201 (1950); U. Frisch and J. Bec, *Burgulence*, in *Les Houches 2000: New Trends in Turbulence*, M. Lesieur, A. Yaglom and F. David, eds., pp. 341-383, Springer EDP-Sciences, 2001